Supplementary Materials

Bubble induced piezoelectric activation of peroxymonosulfate on BiOCl for formaldehyde degradation during absorption process: Density functional theory study

Wenwen Xu [a,b], Binghua Jing [b], Qianyu Li [b,c], Jiachun Cao [a,b], Junhui Zhou [b], Juntian Li [b,c], Didi Li [a], Zhimin Ao [b,a*]

[a] Guangdong-Hong Kong-Macao Joint Laboratory for Contaminants Exposure and Health, Guangdong Key Laboratory of Environmental Catalysis and Health Risk Control, Institute of Environmental Health and Pollution Control, School of Environmental Science and Engineering, Guangdong University of Technology, Guangzhou 510006, PR China.
[b] Advanced Interdisciplinary Institute of Environment and Ecology, Beijing Normal University, Zhuhai 519087, PR China.
[c] School of Environment, Beijing Normal University, Beijing 100875, PR China.
*Corresponding author's email address: Zhimin.ao@bnu.edu.cn.

Pages (4)

Tables (3)

- Table S1. Adsorption energies (E_{ads}, eV), the O-O bond length ($l_{O\text{-}O}$, Å), the S-O bond length ($l_{S\text{-}O}$, Å) of PMS, and the electron transfer (ΔQ, |e|) from BiOCl (001) to PMS under different strains.
- Table S2. The adsorption energies (E_{ad}) of C_6H_6, CH_2Cl_2, and HCHO on BiOCl (001) under different strains.
- Table S3. The reaction energy E_{reac} and energy barrier E_{bar} of each step elemental reaction in degradation of HCHO. Where, 1 represents the degradation process of HCHO by the BiOCl/ $HO^{\bullet}$ system, and 2 represents the direct degradation process of HCHO by $HO^{\bullet}$ radical in the article. The energy unit is kcal/mol.

Figures (6)

- Fig. S1. The biaxial strain configurations of BiOCl (001) from –10% to +10% in the AB direction.
- Fig. S2. (a) Hirshfeld charges of $[Bi_2O_2]^{2+}$ in BiOCl (001) under different strains. (b) Hirshfeld charges of $[Bi_2O_2]^{2+}$ and $2Cl^-$ in BiOCl (001) under uniaxial strains of C direction.
- Fig. S3. (a) The dipole moment of BiOCl 3 × 3 × 1 supercell along the Z axis under biaxial strains of AB direction. (b) Hirshfeld charges of $[Bi_2O_2]^{2+}$ and $2Cl^-$ in BiOCl 3 × 3 × 1 supercell under biaxial strains of AB direction.
- Fig. S4. The adsorption configuration of PMS under the strain of BiOCl (001) from –10% to +10% in the AB direction.
- Fig. S5. The reaction pathway of PMS activation by BiOCl (001) with –8% strain.
- Fig. S6. HOMO-LUMO orbitals of BiOCl (001) with the strain of –8% ~ 10%.

Table S1. Adsorption energies (E_{ads}, eV), the O-O bond length ($l_{O\text{-}O}$, Å), the S-O bond length ($l_{S\text{-}O}$, Å) of PMS, and the electron transfer (ΔQ, |e|) from BiOCl (001) to PMS under different strains.

	–4%	–2%	0	2%	4%	6%	8%
E_{ads} (eV)	–3.4909	–3.3091	–3.2145	–3.0483	–2.9153	–2.8131	–2.8085
$l_{O\text{-}O}$ (Å)	1.4670	1.4680	1.4690	1.4720	1.4730	1.4670	1.4670
$l_{S\text{-}O}$ (Å)	1.7210	1.7300	1.7300	1.7330	1.7290	1.6950	1.7550
ΔQ (|e|)	0.4576	0.4507	0.4578	0.4608	0.4442	0.4342	0.4229

Table S2. The adsorption energies (E_{ad}) of C_6H_6, CH_2Cl_2, and HCHO on BiOCl (001) under different strains.

Strain / E_{ads} (eV)	–4%	–2%	0	2%	4%	6%	8%
HCHO	–0.53	–0.50	–0.48	–0.45	–0.40	–0.41	–0.48
C_6H_6	–0.18	–0.22	–0.25	–0.28	–0.29	–0.42	–0.51
CH_2Cl_2	–0.27	–0.28	–0.28	–0.30	–0.32	–0.36	–0.49

Table S3. The reaction energy E_{reac} and energy barrier E_{bar} of each step elemental reaction in degradation of HCHO. Where, 1 represents the degradation process of HCHO by the BiOCl/ $HO^{\bullet}$ system, and 2 represents the direct degradation process of HCHO by $HO^{\bullet}$ radical in the article. The energy unit is kcal/mol.

Elemental reaction		1		2	
		E_{reac}	E_{bar}	E_{reac}	E_{bar}
Step 1	$HCHO + HO^{\bullet} \rightarrow {}^{\bullet}CHO + H_2O$	–61.16	0	–30.92	0
Step 2	${}^{\bullet}CHO + HO^{\bullet} \rightarrow HCOOH$	–154.46	0	–48.24	0
Step 3	$HCOOH + HO^{\bullet} \rightarrow {}^{\bullet}COOH + H_2O$	–95.11	0	–21.85	2.16
Step 4	${}^{\bullet}COOH + HO^{\bullet} \rightarrow CO_2 + H_2O$	–61.90	0	–120.59	0
Step 1	$HCHO + HO^{\bullet} \rightarrow {}^{\bullet}CHO + H_2O$	–61.16	0	–30.92	0
Step 2	${}^{\bullet}CHO + HO^{\bullet} \rightarrow HCOOH$	–154.46	0	–48.24	0
Step 3	$HCOOH \rightarrow CO + H_2O$	20.21	69.01	19.25	65.81

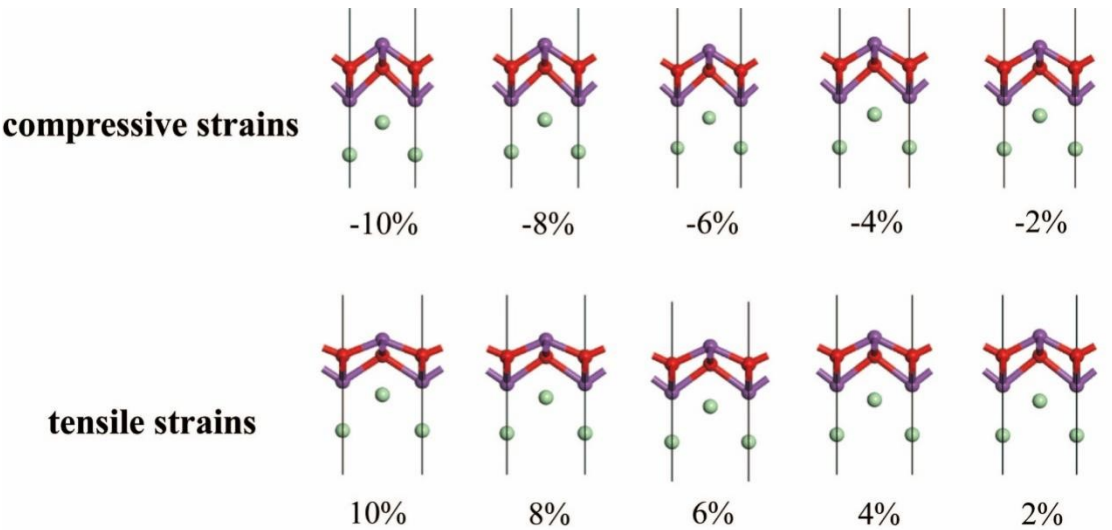

Fig. S1. The biaxial strain configurations of BiOCl (001) from –10% to +10% in the AB direction.

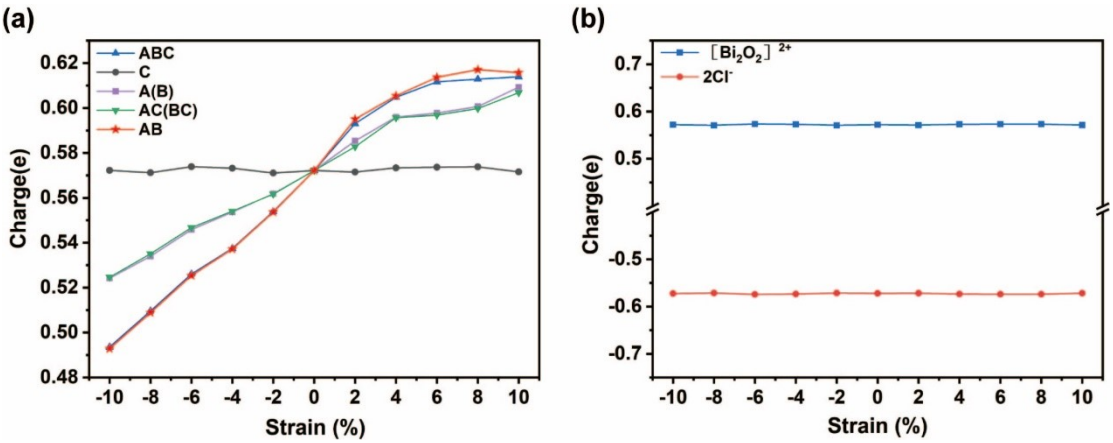

Fig. S2. (a) Hirshfeld charges of $[Bi_2O_2]^{2+}$ in BiOCl (001) under different strains. (b) Hirshfeld charges of $[Bi_2O_2]^{2+}$ and $2Cl^-$ in BiOCl (001) under uniaxial strains of C direction.

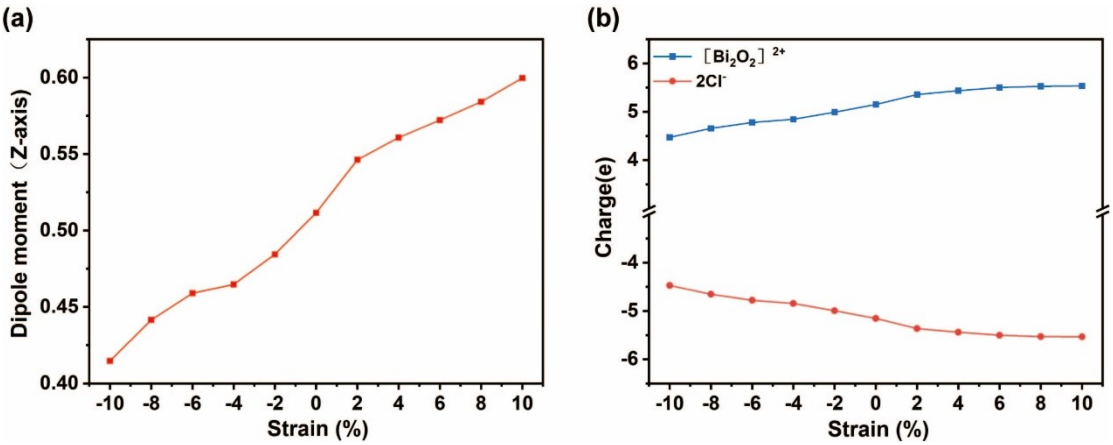

Fig. S3. (a) The dipole moment of BiOCl 3 × 3 × 1 supercell along the Z-axis under biaxial strains of AB direction. (b) Hirshfeld charges of $[Bi_2O_2]^{2+}$ and $2Cl^-$ in BiOCl 3 × 3 × 1 supercell under biaxial strains of AB direction.

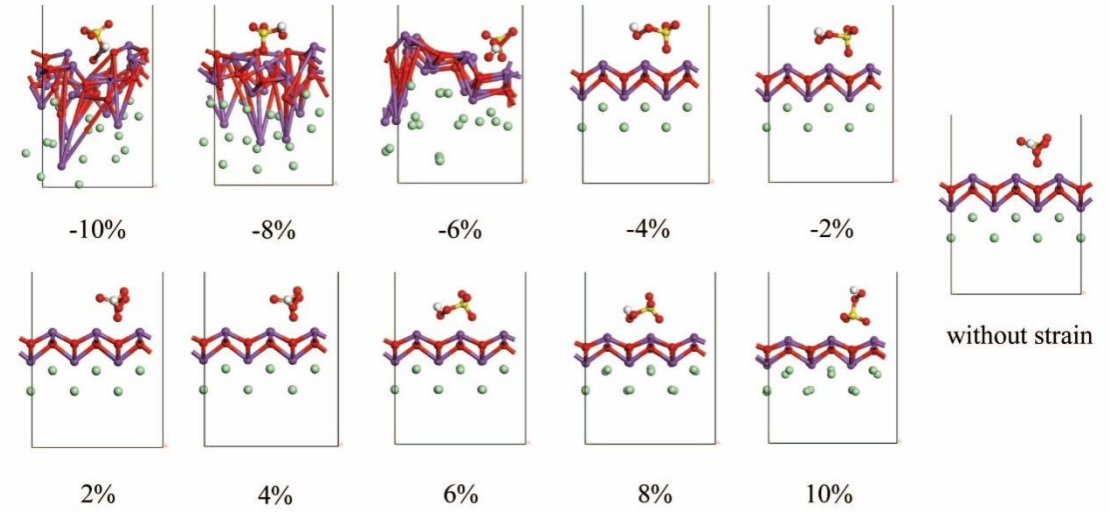

Fig. S4. The adsorption configuration of PMS under the strain of BiOCl (001) from –10% to +10% in the AB direction.

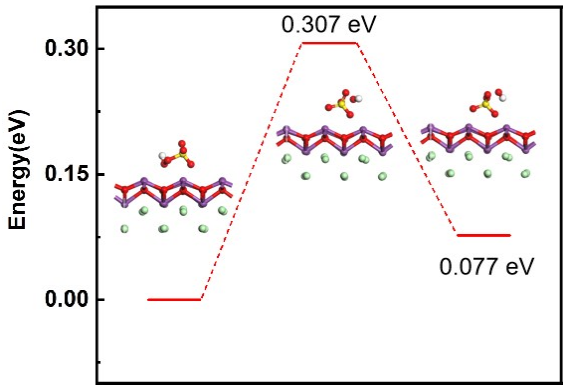

Fig. S5. The reaction pathway of PMS activation by BiOCl (001) with –8% strain.

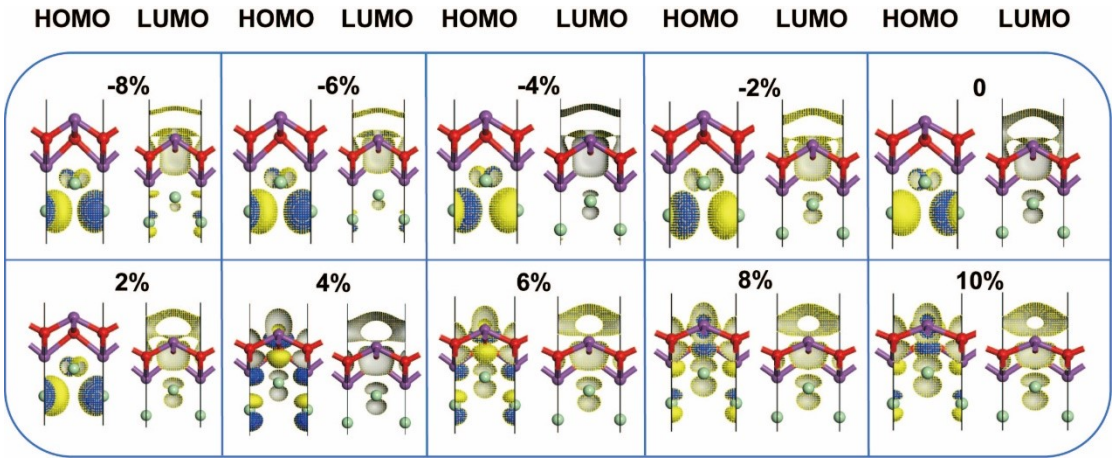

Fig. S6. HOMO-LUMO orbitals of BiOCl (001) with the strain of –8% ~ 10%.